Footprint Catalysis. V.[1—4] Substituent Effects of Template Molecules on the Catalytic Behavior of Imprinted Molecular Footprint Cavities

Toyoshi SHIMADA, Ritsuko KURAZONO, and Kensaku MORIHARA*
Department of Chemistry, Faculty of Science, Nara Women's University, Kitauoyanishi-machi, Nara 630
(Received September 7, 1992)

"Footprint catalysts" are silica(alumina) gel catalysts with tailored substrate specificities; they are easily prepared by the present authors' molecular imprinting procedures with an appropriate template. Four footprint catalysts were newly prepared by imprinting using *p*-acetamido-substituted derivatives of benzenesulfonamide and benzamide as templates. They catalyzed transacylations of benzoic anhydride and 4-(acetamido)benzoic benzoic anhydride, respectively. The effects of the acetamido substituents apart from the reaction center on the substrate specificities were investigated.

We have developed an imprinting method for the design of special silica(alumina) gel catalysts with tailored substrate specificities.[1—6] The present authors' molecular imprinting procedure with an appropriate template can prepare these catalysts from commercially available silica gel. Their catalytic sites are "molecular footprint"-like cavities on the gel surface.

A catalytic cavity comprises the complementary structures to the template molecule used in the molecular imprinting and a Lewis acid site (Al atom isomorphically substituted into the silicate matrix) in the bottom of the cavity. The substrate specificities of the catalytic cavities depend on their complementary structures.

Previous papers in this series reported that the complementary structures neighboring the acid site directly affect the catalytic behavior of the Lewis acid site to originate some enzyme-like catalytic features. They were susceptible to competitive inhibition with compounds resembling the substrate's molecular shape; the cavities tetrahedrally imprinted with a phosphonamide derivative revealed a large rate enhancement by stabilizing the tetrahedral intermediate of the reaction;[4] the chirally imprinted cavities exhibited enantioselective catalyses, etc.[5,6] However, the effects of other complementary structures apart from the acid site on the catalysis are still not elucidated.

The present report is concerned with these effects: Four footprint cavities were newly imprinted using *p*-acetamido-substituted derivatives of benzenesulfonamide and benzamide as templates. Their catalyses on the corresponding specific substrate, 4-(acetamido)-benzoic benzoic anhydride, and on benzoic anhydride were investigated by evaluation of their kinetic parameters, k_{cat}, K_m, and k_{cat}/K_m.

Experimental

Materials. All of the chemicals were of guaranteed grade from Nacalai Tesque Co., Ltd., if not otherwise specified.

Templates and Inhibitors: *N*-Benzoylbenzenesulfonamide ($PhCONHSO_2Ph$),[1] **1**, Mp 148°C (lit, 147°C); (Found: C, 59.51; H, 4.26; N, 5.37%).

N-Benzoyl-4-(acetamido)benzenesulfonamide, (*p*-(Ac-NH-)C_6H_4-SO_2-NH-Bz),[2] **2**, Mp 257°C; IR (KBr) 3315 and 3274 (-NH-), 1674 (C=O), 1538 (amide I), 1354, and 1165 cm^{-1} (S=O); ^1H NMR ($CDCl_3$) δ=7.22 (m, 9H, ArH) and 1.47 (s, 3H, CH_3-); (Found: C, 56.47; H, 4.32; N, 9.28%).

4-(Acetamido)benzenesulfonamide,[2] **3**, Mp 219.5°C (lit, 219°C); (Found: C, 59.11; H, 8.00; N, 9.28%).

4-(Acetamido)benzamide, **4**, Mp 277—278°C; IR (KBr) 3270 (-NH-), 3243 (NH_2), 1650 (C=O), and 1540 cm^{-1} (amide II); ^1H NMR (DMSO-d_6) δ=7.50—7.89 (m, 4H, ArH) and 2.19 (s, 3H, CH_3-); (Found; C, 60.69; H, 5.48; N, 15.80%).

Benzamide, **5**, Benzenesulfonamide, **6**, and Acetanilide, **7**, were of guaranteed grade from Nacalai Tesque Co., Ltd. and were used without further purfication.

Silica Gel : Merck Kieselgel 60, art. no. 7754, particle size 0.06—0.20 mm, mesh 70—230, was used.

Substrate : Benzoic anhydride, **8**, was recrystallized from benzene–petr. benzine, Mp 42°C.

4-(Acetamido)benzoic benzoic anhydride (*p*-(Ac-NH-)-C_6H_4-CO-O-Bz), **9**, was prepared according to the usual procedure for mixed anhydrides synthesis in peptide chemistry. 4-(Acetamido)benzoic acid (Mp 271—272°C) (8.95 g) and triethylamine (5.05 g) were dissolved in dichloromethane (50 cm^3), and to this solution was added benzoyl chloride (7.03 g) portionwise within 25 min with vigorous stirring below 0°C, and the reaction was run for an additional 3 h. To the mixture was then added benzene (50 cm^3) to precipitate and remove the triethylamine salt by filtration. The filtrate was concentrated to a syrup with the salt formed being removed again. The syrup, by addition of petroleum benzine, solidified to give a crude product, Mp 98—100°C. Repeated recrystallization from ethyl acetate-petroleum benzine yielded a pure product, Mp 113—114°C, yield 65%. IR (KBr) 3324 (-NH-), 1779, 1712 (C=O anhydride), 1678 (C=O amide I), 1598 (C=C arom.), 1536 (amide II), 1453, 1373 (CH_3-), 1226 (C-O-C amide III), 709, and 700 cm^{-1} (C-H arom.); ^1H NMR ($CDCl_3$-DMSO-d_6=6 : 1) δ=10.0 (s, 1H, -NH-), 8.15—7.53 (m, 9H, ArH), and 2.18 (s, 3H, CH_3-); (Found: C, 67.40; H, 4.67; N, 5.08%).

Nucleophile : Potassium 2,4-dinitrophenolate, prepared and recrystallized as previously reported,[3] was dissolved in acetonitrile with the aid of 18-crown-6 to 5.0×10^{-3} mol dm^{-3}.

Catalysts. Four imprinted catalysts and one control catalyst were prepared from Merck Kieselgel 60 according to the imprinting procedure previously described.[3,4] The outline of the imprinting procedure is summarized as follows; the silica gel (100 g) was refluxed with concd hydrochloric acid for 4 h to release the surface silanol groups. After washing with water, an aluminium chloride aqueous solution (0.2 mol dm^{-3}, 50 cm^3) was added to the acid-treated silica gel and then the mixture was allowed to soak for two days at pH 7.0—8.0. To this gel was added the template molecule **1** (or **2**—**4**) (2.0×10^{-3} mol per 10 g of gel) in acetone (20—50 cm^3). The supernatant was acidified to pH 4.0 quickly, and the mixture was allowed to stand for 1 week at room temperature. It was then air-dried at room temperature for 1 week. The gel was subjected to methanol extraction to remove the template molecule. Molecular footprint-like cavities with catalytic ability were formed on the surface of the silica(alumina) gel (the cavities imprinted with template **1**, **2**, **3**, and **4** are hereafter referred to as {**1**}, {**2**}, {**3**}, and {**4**}, respectively). The control catalyst stemmed from the aluminium ion-doped gel and lacked only imprinting with a template; it possessed native Lewis acid sites without any cavity structure. Acid strength determination and Lewis acid detection were carried out by the method of Benesi with Hammett indicators,[1] and by that of Pine and Hagg with phenolphthalein.[1] Catalytic site titration was done according to the pyridine poisoning procedure previously described.[3]

Kinetic Measurement. The reaction conditions and assay system were the same as in previous studies:[3] The reaction mixture comprises an acetonitrile solution of the anhydride substrate (50 cm^3, 1.67×10^{-3} mol dm^{-3}), catalyst (50 mg), and a nucleophile solution (1.0 cm^3). To the substrate solution with a catalyst preequilibrated at 30°C for 10 min, was added the nucleophile to start the reaction which was followed by changes in absorbance at 400, 430, and 500 nm through triple-wave length photometry using a Shimadzu UV-160 spectrophotometer. The pseudo-first-order rate constants were calculated from a semi-log plot of time vs the decrease in optical density at 430 nm. In inhibition studies, the catalyst was kept in contact with an inhibitor in acetonitrile for 1 h at 30 °C, and then equilibrated with a substrate solution for 5—10 min. Following procedures were the same as those mentioned above. Kinetic parameters, K_ms, $k_{obsdmax}$s ($=V_{max}$s in Michaelis–Menten Kinetics) were obtained from Lineweaver–Burk plots through a least squares method, and k_{cat}s were calculated from the $k_{obsdmax}$s by dividing with catalytic sites titers.[3]

Results and Discussion

Characterization of Molecular Footprint Cavities. Competitive inhibition studies using inhibitors with partial structures of template molecules were first carried out to define both the location of the Lewis acid site in a cavity {**2**} and the features of neighboring substructures around the acid site (Fig. 1). Figure 2 shows typical competitive inhibition plots for 2,4-dinitrophenolysis of benzoic anhydride **8** catalyzed over {**2**}, wherein the inhibitors **1**, **2**, **5**, and **6** are used, respectively. The observed coincidence of the intercepts of the Lineweaver–Burk plots on the coordinate axis proves that all the inhibitors bind to the same catalytic sites in spite of their different structures. This finding makes it possible to compare the affinities of

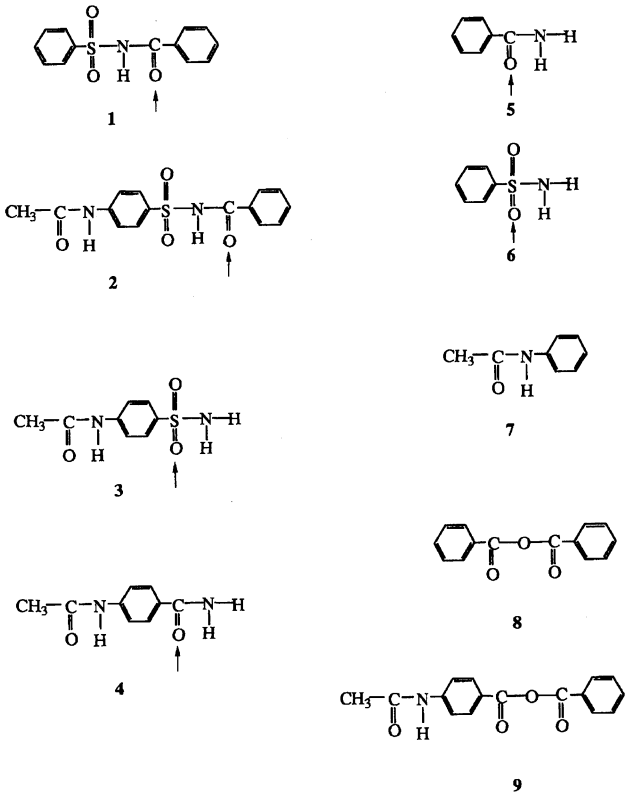

Fig. 1. Template molecles, inhibitors, and substrates. The arrows indicate the location of a Lewis base site in the template molecules.

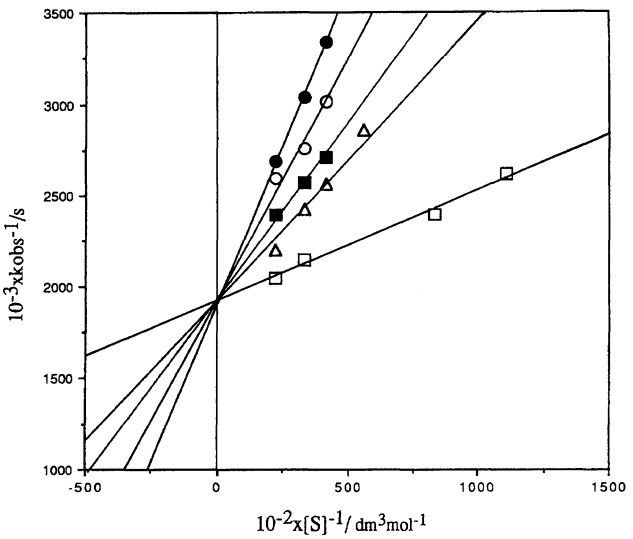

Fig. 2. Competitive inhibition of footprint catalyst {**2**} by **1**, **2**, **5**, and **6**. [S]: benzoic anhydride concentration. [I]: inhibitor concentration. □: [I]=0, ○: [I]=1.0×10^{-5} dm^3 mol^{-1} (**1**). ●: [I]=1.0×10^{-5} dm^3 mol^{-1} (**2**). ■: [I]=1.0×10^{-5} dm^3 mol^{-1} (**5**). △: [I]=1.0×10^{-5} dm^3 mol^{-1} (**6**).

these inhibitiors for the cavity {**2**} by the term $-\Delta G^0_{ass}$ ($=RT \ln K_i^{-1}$). The magnitudes of the affinities of the inhibitors for {**2**} are in the order **2**>**1**>**5**>**3**>**6** as Table 1 shows.

The order **5**>**6** disclosed the counterpart of the Lewis acid site in the template molecule **2**. The previous paper reported that the geometry around a Lewis acid in {**1**} could precisely differentiate the sp^2 configuration of bound molecules from their sp^3 configuration.[5] This was because {**1**} might not have a tetrahedrally marked space, but a plane space around the Lewis acid sites. According to the observed order **5**>**6**, the partial structures for the –NHCOPh moiety of {**2**} might prefer **5** with a carbonyl group with an sp^2 configuration to **6** with a sulfonyl group with an sp^3 configuration to fit in them. So, the carbonyl O atom in **5** indicated by the arrows in Fig. 1 must be the counterpart of the Lewis acid site. Such fitting of **5** in {**2**} makes an acid-base complexation without steric strain via the carbonyl O atom in **5** and the Al atom of the Lewis acid site.

Similar consideration that {**3**} shows inhibition by **3**[7] ($K_i = 3.61\times10^{-6}$ mol dm^{-3}) and {**4**} shows inhibition by **4**[7] ($K_i = 2.73\times10^{-4}$ mol dm^{-3}) and that both {**3**} and {**4**} show no inhibition with **7**[7] suggests that the counterpart of **1** is also the carbonyl O atom, that of **3** is the sulfonyl O atom, and that of **4** is the carbonyl O atom of the benzamido group, respectively.

The order **2**>**1**>**5** gives a clue for the estimation of the partial molecular recognition capabilities of the partial structures of {**2**}. These three inhibitors all contain a benzamide moiety, of which the potential affinities for {**2**} must be identical. The observed differences of affinities among **1**, **2**, and **5** for {**2**} are attributable to the affinities of the acetamido and benzenesulfonyl moieties for the corresponding substructures of {**2**}. The $-\Delta\Delta G^0_{(1—5),ass}$ of 0.86 kJ mol^{-1} shows the affinity for the benzenesulfonyl moiety, and $-\Delta\Delta G^0_{(2—1),ass}$ of 0.91 kJ mol^{-1} shows the affinity for the acetamide moiety. These facts prove that even partial structures remote from the Lewis acid site, such as the complementary structures for the acetamide moiety in {**2**}, reveal characteristic molecular recognition capability. However, the values of their affinities are too small compared with that of whole molecular recognition. This reason is explainable based on the following assumption: there is less translational entropy to overcome in the formation of the two-body complex (**2** over {**2**}) than in the formation of the three-body complex (CH_3CONH_2 plus **1** over {**2**}). It is likely to underestimate a $-\Delta\Delta G^0_{(2—1),ass}$ value of a difference between a $-\Delta G^0_{2,ass}$ value and a $-\Delta G^0_{1,ass}$ value, since a $-\Delta G^0_{2,ass}$ value is presumably smaller than the sum of a $-\Delta G^0_{2,ass}$ value and $-\Delta G^0_{1,ass}$ value. In the precise expression, therefore, 0.91 and 0.86 kJ mol^{-1} are the lower limits of each affinity of an acetamide moiety and a benzenesulfonyl moiety, respectively (Scheme 1).

Table 1. K_i values and the Affinities of Inhibitors to {**2**} for the Reaction toward Substrate, **8**, Catalyzed by {**2**}

Inhibitors	K_i[a] / dm^3 mol^{-1}	$-\Delta G^0_{ass}$ / kJ mol^{-1}	$-\Delta\Delta G^0_{(2—1),ass}$ / kJ mol^{-1}
1	3.23×10^{-6}	31.85	
2	2.25×10^{-6}	32.76	0.91
3	4.68×10^{-6}	30.92	
5	4.54×10^{-6}	30.99	
6	6.81×10^{-6}	29.97	

a) K_i indicates the average of the K_i measured in each case.

The Substituent Effects on Substrate Specificities. Four molecular footprint cavities were imprinted with the templates, **1**, **2**, **3**, and **4**, respectively. In this study, benzoic anhydride **8** and 4-(acetamido)-benzoic benzoic anhydride **9** served as the substrates of their catalyzed reactions. The *p*-acetamido substituent in **9** possesses the character of a hydrogen donor and acceptor to make a strong interaction with the silicate matrix; it has a Hammett substituent constant of zero, which means that the two carbonyl carbon atoms in **9** have the same basicity. In the catalysis, the binding mode of **9** over {**2**} might be definitive: this binding places the *p*-acetamido substituent of **9** onto the com-

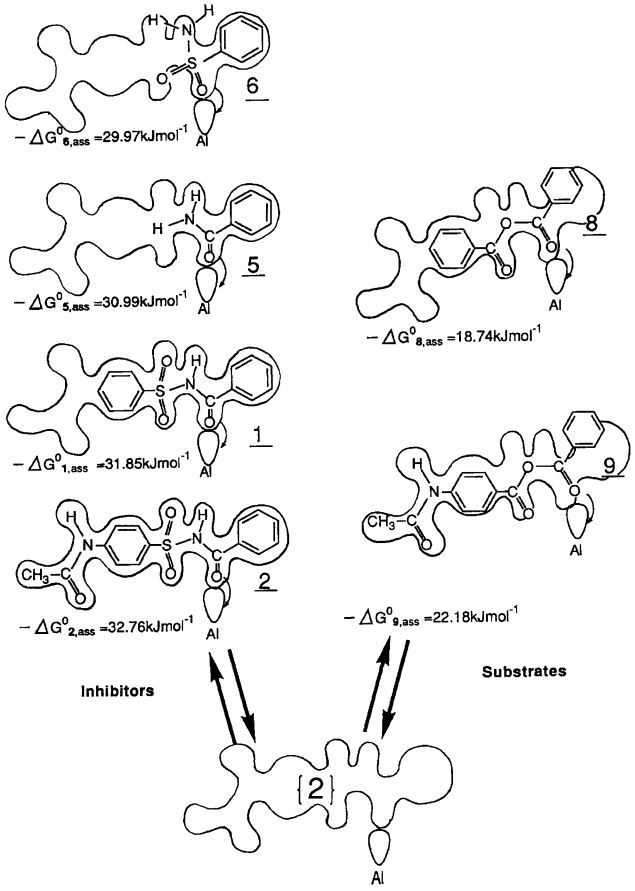

Scheme 1.

Table 2. Kinetic Parameters of the Catalyzed Reactions by Footprint Catalysts

Catalyst imprinted with { }	Substrate	$10^4 \times K_m$ / dm^3 mol^{-1}	(K_m)[a]	$-\Delta G^{0}$[b] / kJ mol^{-1}	$-\Delta\Delta G^{0}$[c] / kJ mol^{-1}	$10^{-2} \times k_{cat}$[d] / dm^{-3} mol s^{-1}	$10^{-5} \times k_{cat}/K_m$ / dm^{-6} mol^2 s^{-1}	(k_{cat}/K_m)[a]
{1}	Bz_2O	3.36	(0.19)	20.15	−1.50	4.04	12.02	(3.19)
	p-(Ac-NH–)C_6H_4COOBz	6.09	(0.32)	18.65		5.45	8.95	(1.34)
{2}	Bz_2O	5.88	(0.33)	18.74	3.44	3.19	5.43	(1.44)
	p-(Ac-NH–)C_6H_4COOBz	1.50	(0.08)	22.18		4.45	30.33	(4.53)
{3}	Bz_2O	15.77	(0.88)	16.25	4.08	4.29	2.72	(0.72)
	p-(Ac-NH–)C_6H_4COOBz	3.13	(0.16)	20.33		3.80	12.14	(1.81)
{4}	Bz_2O	11.40	(0.63)	17.07	3.06	5.84	5.12	(1.36)
	p-(Ac-NH–)C_6H_4COOBz	3.39	(0.18)	20.13		5.96	17.58	(2.62)
Control	Bz_2O	18.00	(1.00)	15.92	−0.16	6.79	3.77	(1.00)
	p-(Ac-NH–)C_6H_4COOBz	19.20	(1.00)	15.76		12.87	6.70	(1.00)
{$PhPO(NHBz)_2$}[e]	Bz_2O	4.06	(0.23)	19.36		33.36	82.23	(21.81)

a) Figures in parentheses mean normalized values obtained by dividing with the corresponding values of the control catalyst. b) Standard free energy change in the binding step ($-\Delta G^0 = RT \ln K_m^{-1}$). c) The differences of the affinities between $-\Delta G^0_{\mathbf{9},ass}$ and $-\Delta G^0_{\mathbf{8},ass}$. d) Calculated with the molarities of catalytic sites per g determined by titration using pyridine poisoning. e) These data are quoted from a previous paper (Part IV).

plementary structures in {**2**} that correspond to the *p*-acetamido moiety of **2** to make the maximum interaction between **9** and {**2**}. Another reversed (tail to head) binding mode is unlikely, because it should cause much steric hindrance. These character and definitive binding modes would make it clear and simple to investigate the substituent effects of the *p*-acetamido group in **9** on the substrate specificities. Their kinetic parameters are shown in Table 2.

K_m values can serve as a measure for the affinity of a cavity to a substrate, assuming they are nearly equal to the association constants of the cavities to the bound substrate molecules. As shown in Table 2, the native catalytic sites of the control catalyst exhibit almost identical K_m values for **8** and **9**, respectively, which implies that they cannot differentiate the two substrates. However, all the imprinted catalytic cavities showed larger affinities than that of the control catalytic sites; they simultaneously exhibited remarkable differences between the K_m values for **8** and **9**, respectively. They demonstrated clear substrate specificities in the binding step of the catalysis. These specificities must originate from the affinities of the *p*-acetamido substituent of **9** to the corresponding complementary structures in the cavities. The magnitude of the affinities due to the *p*-acetamido moiety is separately obtainable by subtraction, $-\Delta\Delta G^0_{(\mathbf{9}-\mathbf{8}),ass} = \Delta G^0_{\mathbf{9},ass} - \Delta G^0_{\mathbf{8},ass}$; they are −1.5 kJ mol^{-1} for {**1**}, 3.44 kJ mol^{-1} for {**2**}, 4.08 kJ mol^{-1} for {**3**}, 3.06 kJ mol^{-1} for {**4**}, and −0.16 kJ mol^{-1} for the native catalytic sites of the control catalyst, respectively. The negative affinity (−1.50 kJ mol^{-1}) for {**1**} is attributable to the exclusion of the *p*-acetamido moiety from the cavity. This value due to the exclusion effect of the cavity structures is significantly large as compared to the value (−0.16 kJ mol^{-1}) for the native surface around the Lewis acid site of the control catalyst that lacks any cavity structures. The positive affinities (3.44, 4.08, 3.06 kJ mol^{-1}) can also be attributed to the correct inclusion of the *p*-acetamido moiety in the corresponding cavity structures. Among them, the affinities of **9** for {**3**} and {**4**} are not intrinsic but apparent: the binding of **9** to {**3**} and to {**4**} causes not only the inclusion of the *p*-acetamido moiety in the cavities, but also the exclusion of the benzoyl moiety of **9** from the cavities. The inclusion effects of the *p*-acetamido moiety are strong enough to overcome the exclusion effects, though the *p*-acetamido moiety locates remote from the Lewis acid site. The intrinsic affinities, therefore, should be larger than the apparent affinities. However, a similar value (3.44 kJ mol^{-1}) of **9** for {**2**} was observed; it might be brought about only by the inclusion. The *p*-acetamido moiety of **9** is farther from the Lewis acid site in {**2**} in this case than that of **9** on {**3**} and {**4**}, which might result in the similar affinity. These findings about the affinities suggest that the *p*-acetamido substituent which locates even remote from the Lewis acid site distinctly can affect, whether positively or negatively, the binding step of the catalysis, i.e., the K_m values.

As can be seen in Table 2, both the imprinted catalytic cavities and the native catalytic site exhibit narrowly distributed k_{cat} values. The differences observed between the k_{cat} values for **8** and **9** are remarkably smaller than those observed between the K_m values for **8** and **9**.

These findings suggest that the effects of the cavity structures appear not on the catalytic step, but on the binding step of the catalysis. This is because the templates used here (**1**, **2**, **3**, **4**) are not transition state analogues, but reactant-like compounds; the cavities imprinted with them have complementary structures for the substrate in the reactant state of the catalyzed reaction, which should provide such catalysis that shows a substrate specificity in the binding step. If the template

is proper transition state analogue or a reactive intermediate analogue, the cavities imprinted with it can stabilize the transition state or the reactive intermediate in the catalyzed reaction to reduce the activation energy of the catalytic step; such cavities should reveal a catalytic effect on k_{cat}, not on K_m. Indeed, we previously reported such catalytic behaivior of the cavities:[4] A tetrahedral intermediate analogue for **2**, *N*,*N*′-dibenzoyl-*p*-phenylphosphonic diamide ($PhPO(NHCO\text{–}Ph)_2$), marked such cavities that displayed a catalytic effect clearly on k_{cat}, not on K_m, of which data are cited in Table 2 for comparison. Since these two mechanisms of specificity have been observed, the k_{cat}/K_m value should serve as a proper measure for net catalytic specificity, as it usually does in enzyme catalyses.[8]

The k_{cat} values of {**1**}, {**2**}, {**3**}, and {**4**} for **8** and **9** are smaller compared with that of the control; the imprinted cavities show poorer catalytic activities. In spite of these facts, these catalytic cavities sufficiently compensate the unfavorable k_{cat} by the sacrifices of favorable K_ms to result in better catalytic activities (Table 2). Thus the cavity structures contribute to the catalytic activity through high substrate specificity in the binding step.

The favorable effects of the *p*-acetamido moiety on K_m reflect on the k_{cat}/K_m value; the k_{cat}/K_ms of {**2**}, {**3**}, and {**4**} for **9** are 30.33×10^5, 12.14×10^5, and 17.58×10^5 $mol^{-2}\,dm^6\,s^{-1}$, respectively. Their relative ratios over the corresponding control are significantly large, as shown in Table 2, and are comparable to other imprinted cavities thus far investigated.[3,4,6]

Concluding Remarks. The cavity structures for the *p*-acetamido moiety in {**2**}, even if they locate far from the Lewis acid site, play an important role in the catalysis; their effects are especially manifest in the selective process based on the molecular recognition capability. A similar contribution of a binding site for the amide moiety to the catalysis is also observed in the action of a natural enzyme. The binding sites in the active loci of α-chymotrypsin comprise a hydrophobic pocket and a carbonyl group of Ser-214, the latter of which makes a strong interaction with the amide group of a substrate molecule to bring about effective catalysis.[9] In this sense, the present catalytic cavities can serve as a unique enzyme model.

The outstanding features of the molecular footprint cavities are their precise and easily-imprintable molecular recognition capabilities: They can provide a tailor-made catalyst with required specificities, such as enantioselectivities,[5,6] and tailor-made specific adsorbants for affinity chromatography.[7] The most important thing here is how to design proper template molecules for the imprinting. The remarkable effects of a remote substituent of template molecules in the present study would extend the scope of the template design for imprinting cavities with required functions.

The authors would like to thank Dr. Takashi Nakazawa for his helpful advice and NMR measurements.

References

1) Part I: K. Morihara, S. Kurihara, and J. Suzuki, *Bull. Chem. Soc. Jpn.*, **61**, 3991 (1988).
2) Part II: K. Morihara, E. Nishihata, M. Kojima, and S. Miyake, *Bull. Chem. Soc. Jpn.*, **61**, 3999 (1988).
3) Part III: K. Morihara, E. Tanaka, Y. Takeuchi, K. Miyazaki, N. Yamamoto, Y. Sagawa, E. Kawamoto, and T. Shimada, *Bull. Chem. Soc. Jpn.*, **62**, 499 (1989).
4) Part IV: T. Shimada, K. Nakanishi, and K. Morihara, *Bull. Chem. Soc. Jpn.*, **65**, 954 (1992).
5) K. Morihara, M. Kurokawa, Y. Kamata, and T. Shimada, *J. Chem. Soc., Chem. Commun.*, **1992**, 358.
6) T. Matsuishi, T. Shimada, and K. Morihara, *Chem. Lett.*, **1992**, 1921.
7) T. Shimada and K. Morihara, unpublished data.
8) A. Fersht, "Enzyme Structure and Mechanism," Freemen and Co., Ltd., San Francisco (1977).
9) I. V. Berezin, N. F. Kanzanskaya, and A. A. Klyosov, *FEBS Lett.*, **15**, 121 (1971).